SPATIAL CHARACTERIZATION OF SASE-FEL OF SCSS TEST ACCELERATOR*

P. Mercère#, R. Bachelard, M.-E. Couprie, M. Idir, SOLEIL, Gif-sur-Yvette, France
O. Chubar, NSLS-II, BNL, Upton, New York, USA
J. Gautier, G. Lambert, P. Zeitoun, LOA, Palaiseau, France
S. Bucourt, G. Dovillaire, X. Levecq, Imagine Optic, Orsay, France
H. Kimura, H. Ohashi, JASRI/SPring-8, Hyogo, Japan
T. Hara, A. Higashiya, T. Ishikawa, M. Nagasono, M. Yabashi, RIKEN/SPring-8, Hyogo, Japan

Abstract

Spatial characterization of the VUV Self-Amplified Spontaneous Emission (SASE) of the SPring-8 Compact SASE Source (SCSS) Test Accelerator was performed by use of a Hartmann Wavefront Sensor (HWS). The SASE light was characterized for different gains of the Free Electron Laser (FEL), showing that mode selection occurs as closer to the saturation regime of the FEL. The single-shot wavefront measurements were demonstrated to be in good agreement with numerical simulations using GENESIS and SRW propagation code.

INTRODUCTION

Past years saw the fast emergence of VUV Free Electron Lasers such as FLASH (Germany) in the 80-6 nm range [1] and SCSS Test Accelerator (Japan) in the 60-50 nm range [2]. Common particularity of these 4th generation sources stands in their intense, coherent and ultrashort (10-100 fs) light emissions. Numbers of applications such as ultrafast imaging of biomolecules [3, 4] even at atomic scales [5], microscopy-based investigation of matter and development of new imaging methods require these particular light properties, which synchrotron radiation or High-order Harmonic Generation (HHG) in gas cannot completely satisfy. Therefore, FELs appear as complementary sources offering new perspectives. Nevertheless, the associated metrology is essential for a better understanding and optimization of the sources.

Hartmann Wavefront Sensors (HWS) are one way to assess the wavefront properties of a light beam. They are outinely used on synchrotron radiation, FELs and HHG sources [6, 7, 8, 9]. This kind of device is composed by a hole array and a CCD camera. The incident beam passing through the hole array is sampled in many beamlets, eading to individual spots in the CCD plane. The monitoring of each spot position allows then one to assess he incident beam wavefront.

Here, we present the results of a spatial characterization of the SCSS Test Accelerator SASE radiation, which have been carried out with such a device. The HWS has been designed on purpose for this experiment. Wavefront measurements were performed in single-shot and used to assess the optical quality of the beam, the source characteristics, and their shot-to-shot fluctuations.

EXPERIMENTAL SET-UP

The SCSS Test Accelerator is composed by a thermionic pulsed electron gun and an 8 m long C band linear accelerator where the electrons can be accelerated up to 250 MeV [2, 10, 11, 12, 13]. Two in-vacuum hybrid undulator sections (each 4.5 m long) and quadrupoles in between are used for the spatial conditioning of the electron bunch and generation of the SASE radiation. Composed of NdFeB magnets (300 periods of λ_u = 15 mm), the undulators provide a deflection parameter K up to 1.5 for a minimum gap of 3 mm. Several diagnostics including RF Beam Position Monitors (RF-BPM) and Optical Transition Radiation (OTR) screens are available along the beam path for characterization of the electron and light beams during propagation and amplification through the undulator sections. The main routine operation mode of the SCSS FEL is 61.5 nm wavelength with a repetition rate of 30 Hz. Nevertheless for this experiment, the repetition rate of the machine was reduced to 10 Hz in order to allow for single-shot wavefront measurements. Figure 1 shows a sketch of the two undulator sections including Q-poles and diagnostics. The wavefront sensor was placed 17.5 m from the end of the second undulator, behind two 5° grazing incidence Au-coated flat mirrors.

The HWS design was optimized for the requirements of the related experiment, presenting a λ_{VUV}/125 nm RMS accuracy at the operating wavelength of 61.5 nm. For spatial sampling of the incident beam, we used a hole array made out of a 50-µm thick nickel plate. It was composed of 35×35 holes (each 150 µm size square), spaced by 450 µm and turned by 25° to avoid the overlap of the diffraction from adjacent holes in the measurement plane [14]. The detector was a back-illuminated thinned 16-bit XUV CCD camera (1024×1024 pixels of 13 µm) placed 200 mm behind the hole array. The camera was coupled to a 10 Hz operating fast shutter, and synchronized with the FEL pulse train. A 400-nm thick Sn filter was also used to isolate the fundamental SASE radiation from the higher-order harmonics of the FEL.

*Work supported by the IA-SFS European project and the CLEL contract of the Triangle de la Physique
#pascal.mercere@synchrotron-soleil.fr

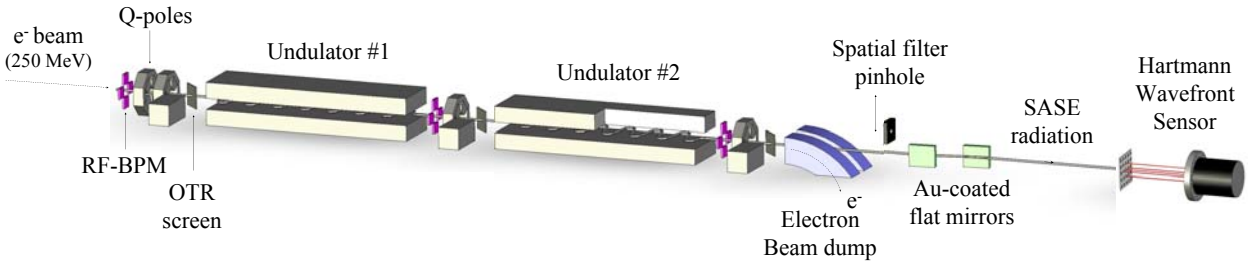

Figure 1: SCSS Test Accelerator undulator sections and experimental layout of the HWS.

WAVEFRONT MEASUREMENT AND ANALYSIS

SCSS was operated at 61.5 nm wavelength, with 250 MeV electrons and the two in-vacuum undulators closed. Figure 2 shows ten single-shot spectra of the fundamental SASE radiation. An intensity of 38 µJ/pulse was measured with a calibrated photodiode. Fluctuation over 3000 shots was estimated of the order of 6% only.

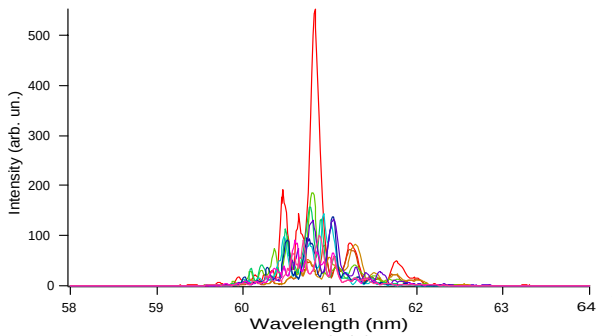

Figure 2: Ten successive single-shot spectra of the fundamental SASE radiation.

The first step of the experiment consisted of the calibration of the wavefront sensor and the two flat deflection mirrors. For this purpose, we used a 50-µm size spatial filter pinhole to generate a perfect spherical reference wave. With the pinhole placed at 13.8 m in front of the wavefront sensor, calibration could be performed on less than half of the diffracted central Airy disk, thus allowing subtraction of the mirrors and assessment of the FEL direct beam absolute wavefront.

Figure 3(a) shows a typical Hartmann pattern of a SASE pulse. The corresponding beam intensity profile (reconstructed from the different spots) is displayed in Fig. 3(b), while Fig. 3(c) shows the residual wavefront aberrations, the so-called optical path difference, obtained after subtraction of the beam paraxial components (i.e. tilts and focus terms). From one shot to the other, we observed slight variations in the beam intensities and sizes at the HWS position. Thus, to ensure relevant analysis and comparison of the wavefront measurements, we used to limit the size of the analysis pupil to $1/e^2$ of the maximum intensity. For a perfect Gaussian beam, this intensity threshold corresponds to 4σ and 86% of the incident flux. As we can see in Fig. 3(c), the wavefront aberrations were measured at 3.11 nm RMS (Root-Mean Square) and 15.7 nm PV (Peak-to-Valley). 0° astigmatism appeared as the main residual aberration component, revealing a slight difference between the horizontal and vertical sources longitudinal positions.

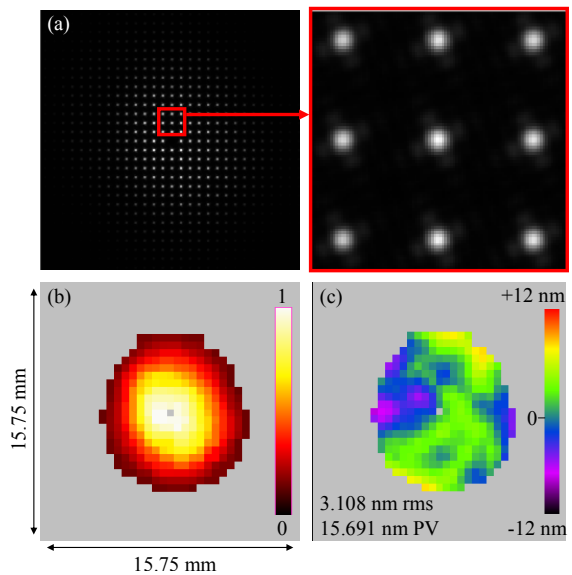

Figure 3: (a) Hartmann pattern of the saturated SASE radiation at 61.5 nm wavelength, with an enlarged part on the spots detected by the CCD – (b) Reconstructed beam intensity profile, and (c) Beam wavefront aberrations.

Over 60 successive single-shot measurements, we could estimate the mean residual wavefront aberrations at 3.7 nm RMS and 17.7 nm PV with respective standard deviations of 0.6 nm and 2.7 nm (Fig. 4).

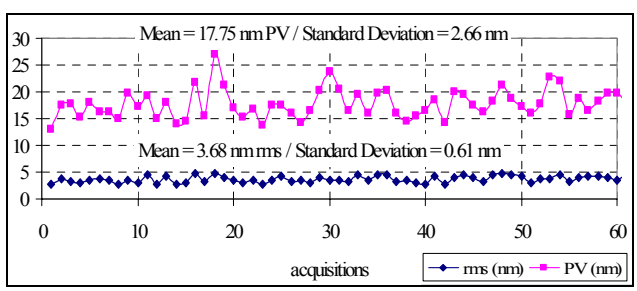

Figure 4: Residual beam wavefront aberrations, in RMS and PV, over 60 successive single-shot measurements.

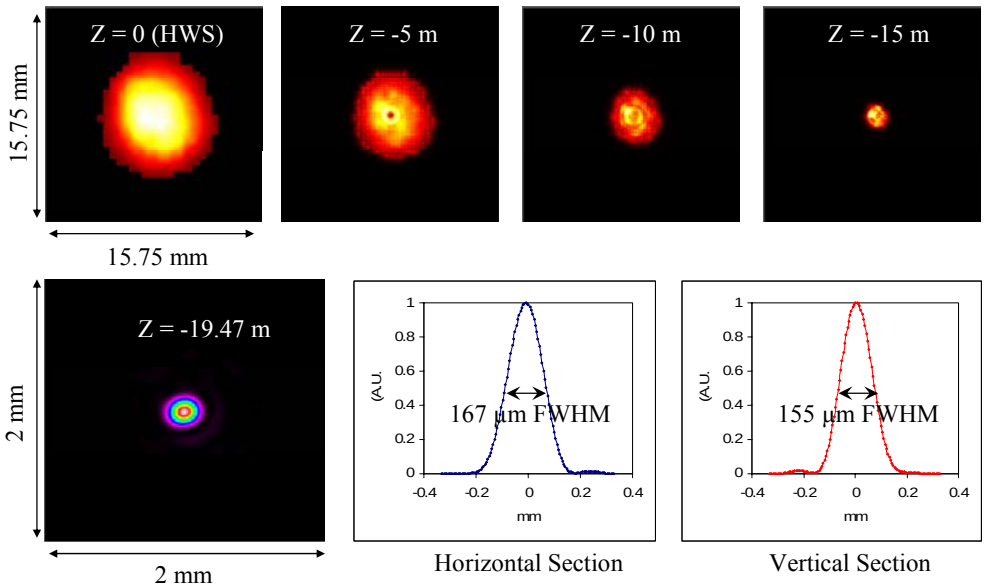

Figure 5: Beam intensity profiles at different distances from the HWS. The electromagnetic field is back-propagated along the beam propagation axis (Z) using *Fourier optics*. Horizontal and vertical cross-sections of the beam are given at the source position.

Knowing both intensity and phase profiles of the beam, the complete electromagnetic field can be back-propagated using Fourier Optics. Figure 5 shows the results of such a back-propagation applied to the experimental measurement given in Fig. 3. We estimated the source to be located 19.47 m distance in front of the HWS (~ 2 m upstream from the exit of the second undulator), leading to a spread of emission half-angle about $\theta_d = 203$ µrad. The source size was estimated to 167 × 155 µm² FWHM, to be convolved with the geometrical dimensions of the source. The horizontal and vertical waists were located respectively 19.68 m and 19.32 m from the HWS, corresponding to 36 cm beam astigmatism.

NUMERICAL SIMULATIONS

Finally, these measurements were compared to numerical simulations, using the FEL emission process of GENESIS 1.3 [16], in combination with the Synchrotron Radiation Workshop (SRW) [17] propagation code. The fundamental radiation was simulated considering an emittance of 1.43 nm.rad, an energy spread of 0.02 %, a peak current of 330 A and a RMS bunch length of 0.18 mm. Wavefront simulations and analysis were performed using the steady-state approach.

Simulation of the intensity growth along the undulator sections shows the usual regimes of lethargy, exponential growth and saturation. Measurements of the energy per pulse with the photodiode after one and two undulator sections are in good agreement with the radiation power simulated by GENESIS 1.3 (Fig. 6(a)). One can also follow the size of the radiation power density (Fig. 6(b)).

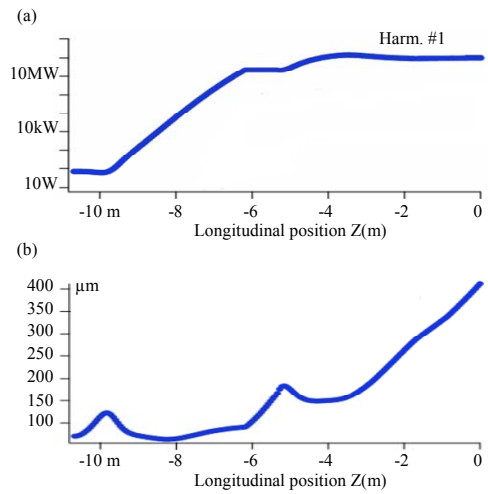

Figure 6: (a) Radiation power and (b) RMS size of the radiation power density distribution vs. the longitudinal position Z along the two undulator sections. The origin Z = 0 is taken at the exit of the second undulator.

Besides, the wavefront propagation implemented in SRW enables to follow the emitted radiation from the exit of the second undulator down to the HWS, and to reconstruct the Hartmann patterns, as illustrated in Fig. 7. The simulated first harmonic and the resulting spots in the HWS detection plane appear in good agreement with the experimental observations. The source could be numerically located ~ 0.8 m upstream from the exit of the second undulator, with a size about 140 × 120 µm² FWHM. The spread of emission half-angle was estimated at θ_d = 197 µrad; and the beam astigmatism at 37 cm distance between the horizontal and vertical waists.

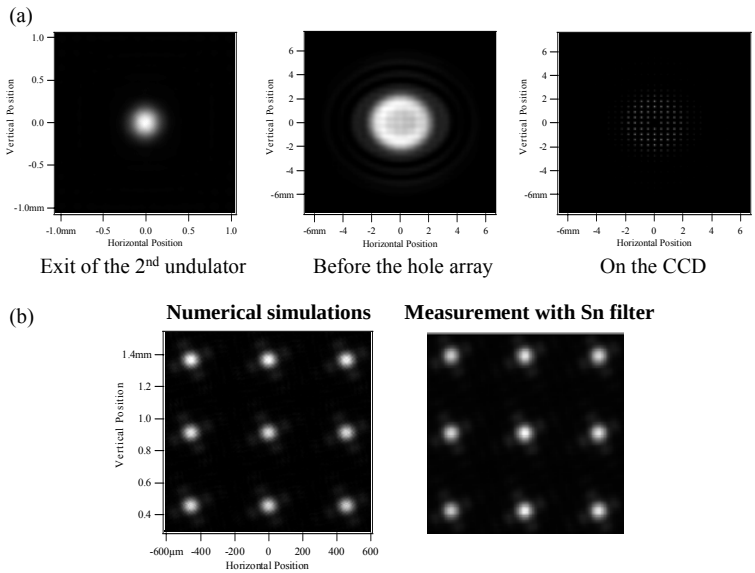

Figure 7: (a) Fundamental SASE radiation as simulated by GENESIS 1.3 and SRW – at the exit of the second undulator, at the hole array position and at the CCD position – (b) Enlarged parts of the simulated and measured Hartmann patterns.

CONCLUSION

We performed single-shot wavefront measurements of the SCSS Test Accelerator SASE light at λ_{VUV} = 61.5 nm. The beam residual wavefront aberrations were measured at 3.7 nm RMS (λ_{VUV}/16) and 17.7 nm PV (λ_{VUV}/3). Fluctuations of aberrations from shot-to-shot were estimated to 16%. However, depending on the machine optimization, the beam optical quality could be improved up to λ_{VUV}/5 PV and λ_{VUV}/22 RMS with shot-to-shot fluctuations about 12% only. We could also characterize the source features (position and size) and the angular spread of emission. Numerical simulations of the SASE emission and the first harmonic propagation lead to results close to our experimental measurements.

REFERENCES

[1] J. Rossbach, Proc EPAC08, Genoa, Italy (2008).
[2] T. Shintake *et al.*, Nat. Phot. 2, 555-559 (2008).
[3] M. Bergh *et al.*, Phys. Rev. E 70, 051904 (2004).
[4] R. Neutze *et al.*, Nature 406, 752 (2000).
[5] I. K. Robinson, Phys. Rev. Lett. 87, 195505 (2001).
[6] P. Mercère *et al.*, Opt. Lett. 28(17), 1534-1536 (2003).
[7] P. Mercère *et al.*, Opt. Lett. 31(2), 199-201 (2006).
[8] M. Kuhlmann *et al.*, Proc. FEL'06, Berlin, Germany (2006).
[9] J. Gautier *et al.*, Eur. Phys. J. D 48, 459-463 (2008).
[10] T. Shintake *et al.*, Nat. Phot. 2, 555 (2008).
[11] T. Shintake *et al.*, Phys. Rev. ST Accl. Beams 12, 070701 (2009).
[12] H. Tanaka *et al.*, Proc EPAC08, Genoa, Italy (2008).
[13] T. Hara *et al.*, Proc APAC 2007, Indore, India (2007).
[14] X. Levecq and F. Harms, "Disposif d'analyse de front d'onde à résolution améliorée", French patent 01 09435 (July 12, 2001), E.C., U.S., and Japan patent extension PCT/FR02/02495 (July 12, 2002).
[15] O. Svelto, Principles of Lasers, 4th, Plenum Press, New York, 1998.
[16] S. Reiche, Nucl. Instr. and Meth. A 429, 243 (1999).
[17] O. Chubar, P. Elleaume, Proc. EPAC98, 1177 (1998).